On the Slow Neutron Absorption Resonances in Iodine

WM. B. JONES, JR.

Cornell University, Ithaca, New York

(Received May 3, 1947)

The 12-channel slow neutron velocity spectrometer at Cornell University is described. Reported here is a measurement with this spectrometer of the neutron cross section of iodine over an energy range extending from 0.0026 to 1000 ev. Below 3 ev, the iodine cross section was found to obey the 1/v absorption law. The total cross section at thermal energy ($kT = 0.025$ ev) was found to be 10.3×10^{-24} cm²/atom. The scattering cross section, found by extrapolating to zero time of flight the straight line which best fitted the data on a cross-section vs. time-of-flight graph, is 3.6×10^{-24} cm²/atom. A single resonance was observed at 20.3 ev. A region containing at least three resonances was observed between 25 and 50 ev. An indication of a resonance or group of resonances was found near 85 ev. An attempt was made to match a symmetrical type Breit-Wigner formula to the observed data at the 20.3 ev resonance. The constants chosen in this manner for the resonance are: $E_r = 20.3 \pm 0.5$ ev, $\sigma_0 = 80 \times 10^{-24}$ cm²/atom with $\sigma_0 > 40 \times 10^{-24}$ cm²/atom, and $\Gamma = 0.45$ ev with $\Gamma < 0.8$ ev. Consideration of the activities for three thicknesses of the absorber for this resonance showed that the absorbers were thick and that $\sigma_0 \Gamma^2 = 15 \times 10^{-24}$ ev² cm²/atom, neglecting the Doppler effect. In the neutron energy region between 25 and 50 ev, the relation between the activity and the absorber thicknesses used showed that the absorbers were thick for the resonances in this region. From the curve of activity as a function of thickness, it was found that $\Sigma_r \, (\sigma_{0r} \Gamma_r^2)^{\frac{1}{2}} = 32.5 \times 10^{-12}$ ev-cm/atom$^{\frac{1}{2}}$ for these resonances, neglecting the Doppler effect. An attempt at fitting two resonances of about equal strength to the data proved to be impossible, and it was concluded that there are three or more resonances in this region. Consideration of the maximum widths of these resonances, that account for the absorption, indicated that the widths were less than 1 or 2 ev. This conclusion is reached regardless of the relation of the level widths to the Doppler width. Therefore, it is believed that there are no resonances for neutron energies between 0 and 70 ev which are so wide as to be incompatible with the present theory of nuclei. Since iodine has only one stable isotope, the resonances observed are for one type nucleus. It would be valuable to know exactly the number of resonances for a wide range of neutron energies; however, the apparatus used in the present experiment does not have sufficient resolution to resolve resonances with a spacing as small as 7 ev at 40-ev energy.

1. INTRODUCTION

THE slow neutron cross section of iodine has been investigated by a number of workers. The earliest measurements were made by indirect methods. Because the resonance absorption in iodine occurs for rather high neutron energies, it has not been possible to determine very accurately by indirect methods the character of the cross section as a function of energy. However, the results of experiments by indirect methods[1] indicated that the resonance-level widths in most nuclei were a few tenths of an electron volt but that the iodine resonance-absorption width was about 15 ev. It was concluded from these experiments that either there is an unusually wide absorption resonance in iodine or there are perhaps several absorption resonances of about equal strengths and with small spacings.

It is much more compatible with theoretical ideas and with much of the experimental data on resonances in various nuclei to attribute the resonance absorption of neutrons by iodine to several closely spaced resonances rather than to one wide resonance. Recently, some experiments of a survey nature with a slow neutron velocity spectrometer[2] indicated that there is one weak absorption resonance in iodine of normal width at 20.6 ev and a region of strong absorption extending from 30 to 45 ev. The wide region of absorption was interpreted as resulting from two absorption resonances, because the measured absorption as a function of energy was not of the shape usually observed for a single resonance. However, even under the assumption of two resonances for this region, one cannot come to the conclusion that the levels are of widths expected from the theory.

In view of the doubt as to the nature of the slow neutron absorption properties of iodine, a more detailed investigation of iodine with a slow neutron velocity spectrometer was indicated. In addition, iodine has only one stable isotope, and

[1] H. A. Bethe, Rev. Mod. Phys. 9, 134 (1937).

[2] C. S. Wu, L. J. Rainwater, and W. W. Havens, Phys. Rev. 71, 175 (1947).

FIG. 1. Block diagram of timing apparatus.
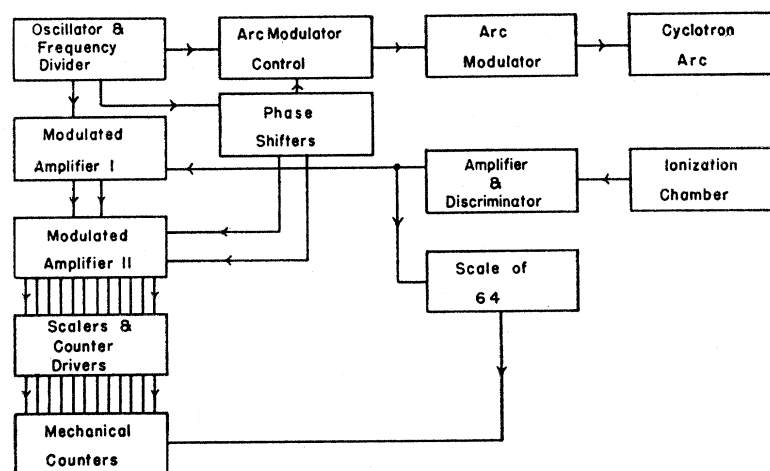
if several resonances were found, information would be obtained on the energy levels in a single nucleus. The experiment to be described here is a study of the neutron cross section of iodine with a slow neutron velocity spectrometer.

2. APPARATUS

The time-of-flight method and an apparatus used for time-of-flight measurements have been described earlier.[3] The apparatus of Baker and Bacher[3] has been improved and expanded by Bacher, Baker, and McDaniel[4] and by McDaniel.[5] The timing equipment used in the present experiment is, with minor improvements the same as that used, but not described, by McDaniel in the measurement of the slow neutron cross section of indium.[5]

The timing equipment of the apparatus is composed of electrical circuits which will turn on the ion source of the cyclotron for a chosen, definite period of time and accurately modulate pulse amplifiers. The cyclotron ion source is an arc type source and will be referred to as the arc. The modulated amplifiers are connected so that certain pulses from the linear amplifier used with the BF_3 ionization chamber are selected. Each modulated pulse amplifier will amplify only those pulses originating from neutrons detected by the BF_3 chamber within a time-of-flight

interval determined essentially by the on-time of the arc, the on-time of the pulse amplifier, and the time separation of these on-times. There are 12 of these modulated pulse amplifiers so that the intensity of the neutron beam in 12 time-of-flight intervals may be measured simultaneously. The cycle of turning on the arc and turning on the modulated amplifiers is repeated at a frequency which is as high as possible without having neutrons produced in one cycle detected in the succeeding cycles.

Figure 1 is a block diagram of the timing equipment. The arrows on the lines connecting the blocks indicate the directions in which the signals proceed between the components of the equipment. In order to simplify the diagram, the cathode-ray oscilloscope and its associated linear sweep circuit, which comprise an important component of the equipment, are not shown. The oscilloscope sweep circuit is so arranged that the sweep may be triggered accurately in any phase with respect to the timing wave which determines the repetition frequency for the equipment. The sweep speed may be adjusted continuously from a speed of 5 μs for a sweep across the screen of the 5-inch cathode-ray tube to a speed of 0.02 second for a sweep across the screen. The sweep speed was calibrated frequently by comparison with the time standard of the equipment. Tap switches are connected so that the vertical deflection plate of the cathode-ray tube may be conveniently connected to any one of the 35 points of the equipment

[3] C. P. Baker and R. F. Bacher, Phys. Rev. 59, 332 (1941).

[4] R. F. Bacher, C. P. Baker, and B. D. McDaniel, Phys. Rev. 69, 443 (1946).

[5] B. D. McDaniel, Phys. Rev. 70, 832 (1946).
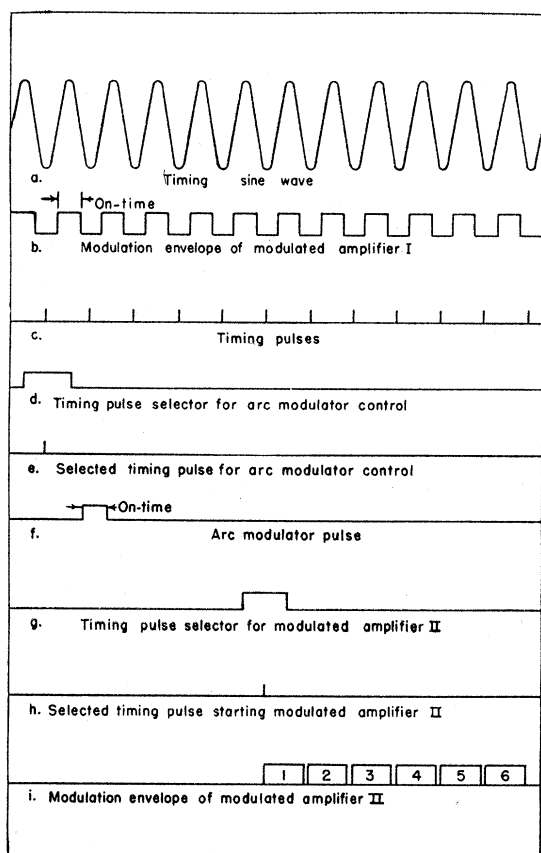
FIG. 2. Timing diagram for timing apparatus.

where there are wave forms which should be viewed in the adjustment and checking of the operation of the equipment.

The time standard is a 100 kc/sec. (± 0.02 percent) crystal oscillator. A six-stage frequency divider is employed to obtain the timing waves of the desired frequencies for determining the on-time of the modulated amplifiers, the time separation of the arc on-time and the on-time of the modulated amplifiers, and the repetition frequency. The timing wave which determines the on-time of the modulated amplifiers has a period twice as long as the on-time. This timing wave will be referred to as the fast timing wave. The detector on-times used in this experiment were 5, 10, 50, and 250 μs corresponding to fast timing wave frequencies of 100, 50, 10, and 2 kc/sec., respectively. The uncertainty in the detector on-times is less than 0.15 μs for the 5 μs on-time and less than 1.5 percent of the on-

time for the longer on-times. The repetition periods used were 300, 320, 400, and 5000 μs.

Figure 2 shows a timing diagram for the operation of the timing equipment during a portion of a repetition period. Reference is made to Figs. 1 and 2 in outlining the operation of the equipment.

The BF_3 ionization chamber gives an electrical pulse upon the detection of a neutron. The pulses from the chamber are amplified by the linear amplifier, and an amplitude discriminator is used to pass only the neutron pulses which are larger than the thermal noise pulses from the amplifier. The rise time of the amplifier is slightly less than 2 μs; this is somewhat greater than the collection time for the electrons in the ionization chamber. The neutron pulses from the discriminator are sent through a pulse shaper which makes all pulses passed by the discriminator of the same size and duration. From the pulse shaper the pulses are sent to a scale-of-64 circuit driving a mechanical counter so that all detected neutrons are counted. From the pulse shaper, the pulses are also sent into the modulated amplifier I which separates the pulses into two sets of timed groups. One set of timed groups is composed of those pulses resulting from neutrons detected in time intervals equal in length to one-half the period of the fast timing wave, and these intervals are separated by a time equal to one-half the period of the fast timing wave. The other set of timed groups of pulses are those not included in the first set of time groups. Figure 2a shows the fast timing wave and Fig. 2b the modulation envelope determining one set of the timed pulse groups.

The low frequency timing wave is sent into phase shifters and from the phase shifters are obtained three pulses which may be adjusted so as to have any desired duration and to start at any desired phase with respect to the low frequency timing wave. Coincidences between these pulses occurring at the repetition frequency and pulses derived from the fast timing wave (shown in Fig. 2c) are used to trigger the arc modulator control and the two sets of 6 modulated amplifiers of modulated amplifier II. Thus the accuracy of all the timing is determined by the fast timing wave.

A selected timing pulse which triggers the arc

modulator control is shown in Fig. 2e. This pulse initiates a linear time sweep in the arc modulator control so the arc may be turned on at a phase which is continuously adjustable over a time interval of about twice the length of a fast timing wave period. This linear time sweep is also used to determine the on-time of the arc. The arc on-time is always made equal to the detector on-time. Figure 2f shows a typical phasing for the arc modulator pulse.

The grouped neutron pulses from modulated amplifier I are sent into modulated amplifier II where certain groups of the pulses are selected to be recorded by the mechanical counters. The selector pulse (Fig. 2g), which selects the fast timing pulse (Fig. 2h) to start one of the chain of 6 amplifiers of modulated amplifier II, may be phased to start the modulation chain with any one of the timing pulses. A chain of the modulated amplifier II selects six successive groups of pulses of one set of the grouped neutron pulses from modulated amplifier I. Thus the neutron pulses appearing in these six time intervals may be recorded on mechanical counters. The other chain of modulated amplifier II selects any six successive groups of pulses of the other set of grouped neutron pulses from modulated amplifier I. Figure 2i shows the modulation envelopes of the amplifiers of one chain. Thus, there are twelve time intervals in which detected neutrons are counted. These twelve time intervals are referred to as the detector channels. The double modulation scheme insures stability and uniformity in the detector channel on-times.

Since the resolving time of the mechanical counters and their driving circuits is relatively large (about 1/30 sec.), it is necessary to use scaling circuits so that no appreciable number of neutron counts will be missed by the recording devices. A scale-of-64 circuit is used with the recorder of the total neutrons detected. A scale-of-4 is used with each of the recorders of the twelve timed intervals.

The neutron source used was the Cornell cyclotron. Deuterons produced by the arc are accelerated in the cyclotron, are brought out of the accelerating region of the cyclotron, and allowed to fall upon a Be target, thus producing neutrons by the (d,n) reaction. The peak deuteron current falling upon the target during the

experimental runs was between the limits of 80 and 150 micro amperes. The target is almost completely surrounded with water, contained in a copper tank, which serves as the moderator for the neutrons. A diagram of the moderator tank is shown in Fig. 3a.

A diagram of the neutron beam collimator and the neutron detector is shown in Fig. 4. The collimator is made up of concentric hollow cylinders of paraffin and B_2O_3 with an especially thick hollow cylinder of B_2O_3 surrounding the BF_3 ionization chamber. This collimation is necessary so that the neutron source will be well defined; i.e., so that neutrons scattered by materials in the cyclotron room will not be scattered into the BF_3 chamber. The collimator is sufficiently effective so that a fast neutron background is detectable only at energies above 100 ev. The BF_3 ionization chamber used as the neutron detector is very similar in construction to the chamber described by Baker and Bacher.[3] The ionization chamber has an effective length of 15 cm and is filled with BF_3 of high purity to
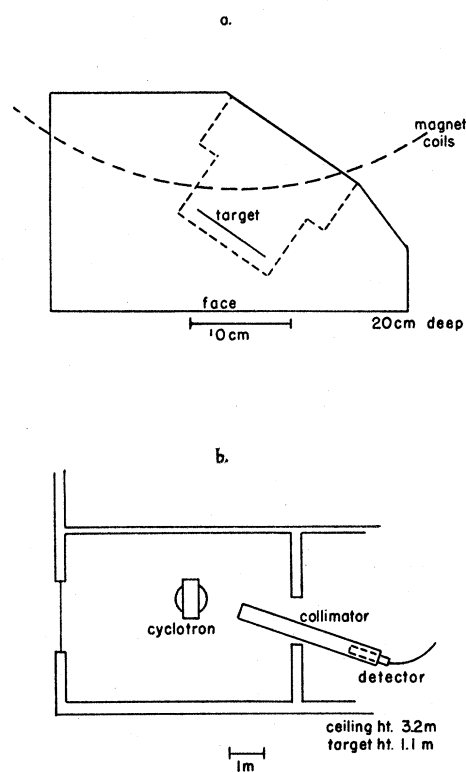
FIG. 3. (a) Moderator tank arrangement, (b) room plan.

a pressure of 2 atmospheres. The chamber collecting potential used is of the order of 3 kv. Figure 3b is a diagram showing the relative positions of neutron source, collimator, and detector.
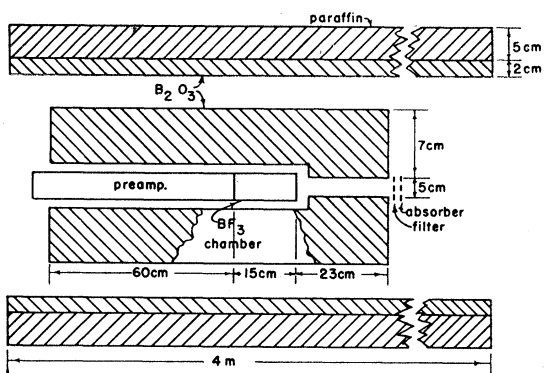
FIG. 4. The neutron beam collimator and neutron detector.

A monitor for the neutron source was used. The monitor neutron detector is a parallel plate ionization chamber in which one plate is coated with uranium. The chamber is filled to a pressure of one atmosphere with argon. This chamber depends on the fission properties of uranium for the detection of slow neutrons. This type chamber is convenient and useful as a slow neutron monitor because of the flat plateaus obtained in counting rate as a function of discriminator bias and as a function of the chamber collecting voltage. During the experiment the monitor chamber was placed directly beneath the moderator tank.

3. EXPERIMENTAL PROCEDURE

The total cross section of iodine as a function of neutron energy was determined by measuring the transmission of samples of iodine of uniform thicknesses as a function of time of flight of neutrons for chosen source-detector distances. In most respects, the procedure for measuring the transmission was similar to that described in the references.[3, 4]

For measurements below 12-ev neutron energy, the source-to-detector distance was chosen to be 3 meters. For measurements above 12 ev, the source-to-detector distance was about 6 meters. The greatest distance used was 6.84 meters, and the exact value of the distance in each of the

high energy runs was determined by the neutron filter which is described below. The distance was measured from the effective position of the source to the effective position of the detector.

The repetition period of the timing equipment was chosen so that neutrons produced in one cycle would not be detected in succeeding cycles. For each repetition period used, it was shown that no significant fraction of the neutrons produced in one cycle was detected in succeeding cycles. This was done by testing with a repetition period much longer than that to be used in the experimental run. With this long repetition period, the detector channels were set to measure the neutron intensities at times of flight equal to the times of flight for recycled neutrons for the repetition period and times of flight of interest for the experimental run. For measurements at neutron energies below 0.6 ev, a repetition period of 5000 μs was used with the source-detector distance of 3 meters. In the energy range 0.6 ev to 10 ev, a thick Cd (0.9 g/cm^2) filter was used which absorbs low energy neutrons, and this allowed a repetition period of 400 μs to be used at the 3-meter source-detector distance without neutron recycling difficulty. Since the average source intensity is proportional to the repetition frequency, *ceteris paribus*, the Cd filter is used to advantage in increasing the channel counting rates. At energies higher than 10 ev, a filter of very thick Cd (3 to 5 g/cm^2) and 1.0 g/cm^2 of In was used. An In absorber of 1.0 g/cm^2 thickness absorbs more than 99 percent of the neutrons with time of flight between 56 and 66 μs/m. If the source-detector distance, d, the repetition period, T_r, and τ_2, a time-of-flight between 56 and 66 μs/m, are chosen for a time-of-flight measurement, τ_1 so that $\tau_1 = \tau_2 - T_r/d$, the recycled neutrons of the first preceding cycle can be removed by a 1.0 g/cm^2 In filter. If recycled neutrons for the other preceding cycles can be removed with another material, such as Cd, an In filter can be used to advantage in making the repetition period short. Such a filter was found feasible for the high energy measurements.

Corrections must be made for the various time lags in the apparatus in order to obtain the exact timing of the neutron time-of-flight intervals from the timing of the various modulation

envelopes observed on the oscilloscope. One correction is the time lag obtained from the fast neutron time distribution function measured with the apparatus. This function will be referred to as the FN-function, and the method of obtaining it is explained below. The FN-function gives the sum of the time lags of the apparatus involved in neutron production and detection. Another correction is the mean time of the neutrons in the moderator. A third type of timing correction is the effect of the variation of the neutron source intensity with energy. This correction is small if the intensity variation is small within the resolution width of the apparatus. The resolution was always made sufficiently good so that this correction was negligible.

To obtain the FN-function, the BF_3 chamber is replaced by a similarly constructed butane filled chamber. Such a chamber detects fast neutrons by detecting the recoil protons. The FN-function is obtained by measuring the fraction of the total neutrons detected which are counted in a detector channel as a function of the time delay of the channel, with respect to the arc modulator pulse. For this measurement, the water is removed from the moderator tank. Not only does the FN-function indicate the time lag, but also

the sharpness of the arc modulation and detection of the neutrons by the equipment. The ideal shape of this function is that of an isosceles triangle with a base twice as long as the on-time. Figure 5 shows a typical FN-function obtained with an on-time of 5 μs. The dotted curve shows the ideal shape of the function. The "tailing" of this function on either side is caused, for the most part, by the finite rise time of the linear amplifier and the straggling in the acceleration of the deuterons in the cyclotron. Thus, for all on-times, the "tailing" is about of the same duration and the FN-function is, therefore, more nearly triangularly shaped for longer on-times. The time lag is taken as the delay of the centroid of this function with respect to the center of the arc modulator pulse. The FN-function was taken at some time during each set of observations, and the delay was always found to be within 0.15 μs of 7.4 μs for the 5 μs on-time and very nearly 7.5 μs for the other on-times used.

For energies above 0.7 ev, the mean time of the neutrons in the moderator is taken as the mean deceleration time, assuming the protons in the water are not bound. For example, this time is 1.5 μs for 1-ev neutrons. At energies below 0.04 ev, the mean time of the neutrons in the moderator is taken as the decay time constant
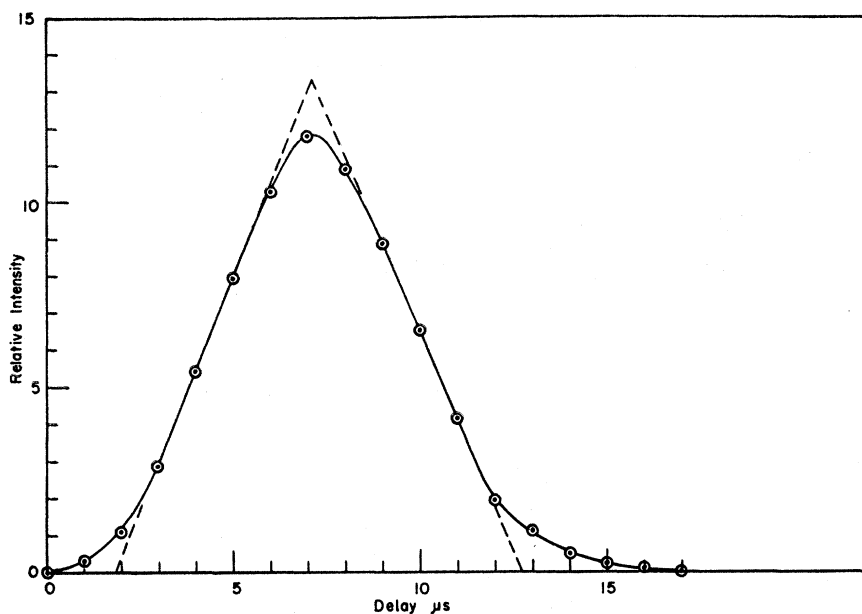
FIG. 5. FN-function or observed time distribution of fast neutrons for 5 μs on-time.

TABLE I. Important features of the experimental conditions.

Run No.	On-time μs	Distance m	Repetition period μs	Source modifier or filter	Absorber thickness g/cm²	Time of flight μs/m	Energy ev
1	250	3	5000	Tray	16.7	490–1420	0.0026–0.0216
2	50	2.97	5000	Tray	31.0	290–477	0.023–0.063
3	50	3	5000	Tray	31.0	98–274	0.0695–0.542
4	10	3	400	0.9 g/cm² Cd	31.0	64–101	0.51–1.28
5	10	3	400	0.9 g/cm² Cd	31.0	23.8–60.6	1.42–9.2
6	5	6.84	300	5 g/cm² Cd 1 g/cm² In	16.2	12.8–20.85	12–31.9
7	5	6.32	300	5 g/cm² Cd 1 g/cm² In	5.96	9.09–17.8	16.5–63.3
8	5	6.32	300	5 g/cm² Cd 1 g/cm² In	2.5	9.09–17.8	16.5–63.3
9	5	6.6	320	5 g/cm² Cd 1 g/cm² In	9.78	5.66–14.0	26.6–164
10	5	6.04	320	3.4 g/cm² Cd 1 g/cm² In	16.2	2.07–11.2	41.6–1200

of the time distribution of neutrons emerging from the moderator. Using water alone as the moderator gave a value for the mean time of 85 μs. Therefore, for measurements in the low energy region, the moderator was modified by placing a sheet of thick Cd directly on the face of the moderator tank to remove the low energy neutrons emerging from the tank and placing adjacent to this a sheet of paraffin 2 cm thick to regenerate low energy neutrons. This paraffin and Cd sheet combination will be referred to as the "tray." The mean time of neutrons emerging from the tray is 30 μs. In the energy region between 0.04 ev and 0.7 ev, it was assumed that the mean time of the neutrons in the tray varied linearly with time of flight from 30 μs at 0.04 ev to 1.8 μs at 0.7 ev.

4. RESULTS

The transmission by several thicknesses of iodine absorbers was measured over the energy interval from 0.0026 ev to 1000 ev, corresponding to a time-of-flight interval from 2.2 μs/m to 1400 μs/m. A resonance was found at 20.3 ev. A region of high cross section was found between 29 and 46 ev, and an analysis shows that this region must contain at least 3 resonances of

about equal strength. Indications of resonances at higher energies were found.

The iodine used for the absorbers was re-sublimed iodine crystals with a minimum purity of 99.985 percent. Brass containers were used for the iodine and a "blank" of brass of the same thickness as the sum of the thicknesses of the two faces of the containers was interposed in the neutron beam when counts were being taken with no absorber. The containers were packed tightly with the iodine in such a way that each absorber was believed to be of uniform thickness.

Table I gives the important features of the experimental conditions under which the data were taken. All the data were corrected for background and time lags. Each separate run is assigned a run number for the purpose of reference. On all graphs showing experimental data, a legend is given which indicates the run number, on-time, source-detector distance, and absorber thickness. Thus the legend "1-250-3m 31 g/cm²" refers to run number one in which the on-time was 250 μs, the source-detector distance was 3 meters, and the absorber thickness used was 31 g/cm².

In the energy range below 10 ev, measurements were made with a resolution which was sufficiently high to detect possible resonances.
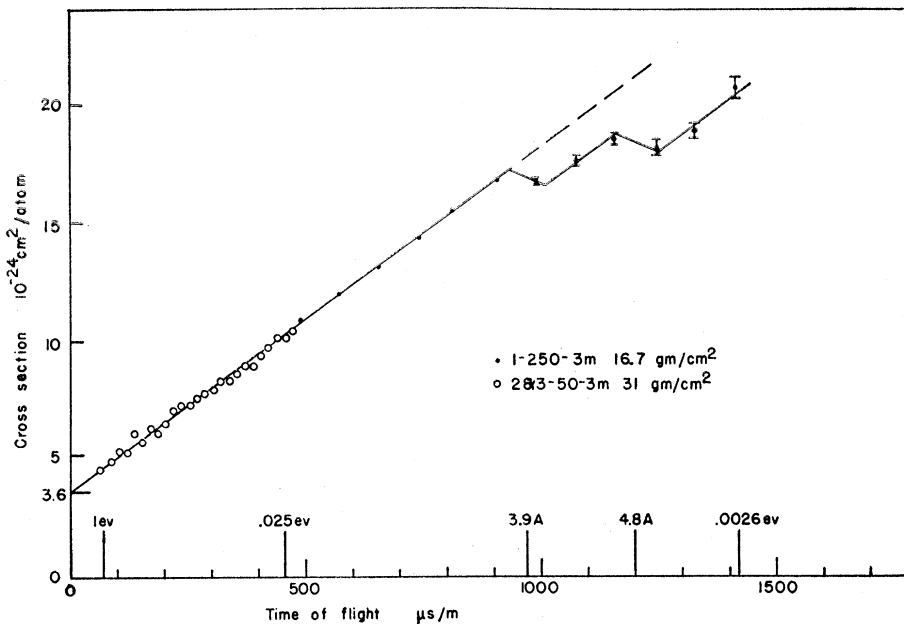
FIG. 6. Low energy neutron cross section of iodine.

Sufficient accuracy was obtained so that the 1/v law would be tested. Figure 6 shows a cross-section plot for times of flight greater than 90 μs/m. The statistical probable errors in the points are indicated by the lengths of the vertical lines through the points, or for those points with no vertical line the probable error is no greater than the diameter of the point. No correction for the effect of the apparatus resolution function on the transmission was made. No such correc-
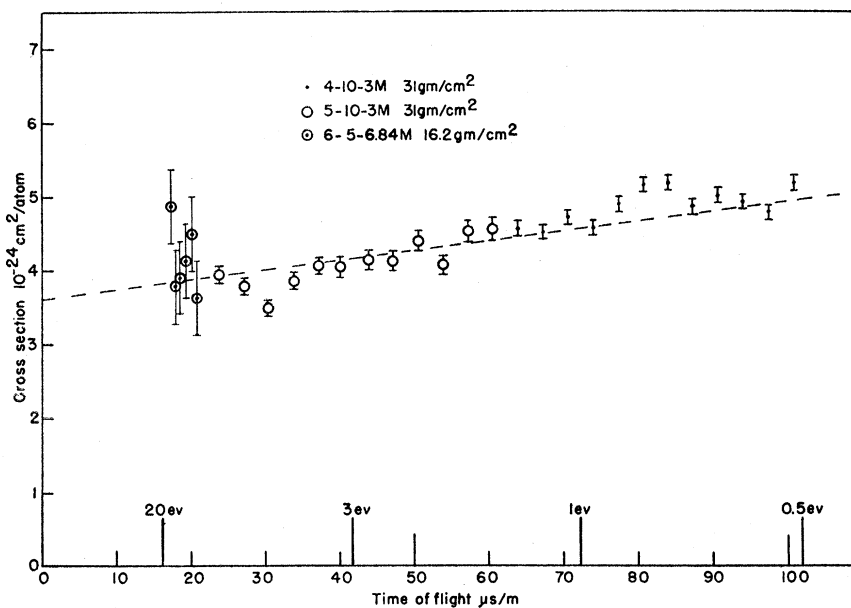
FIG. 7. Neutron cross section of I in the 0.5 to 15-ev region. The dotted line is the best straight line fit for the low energy data.
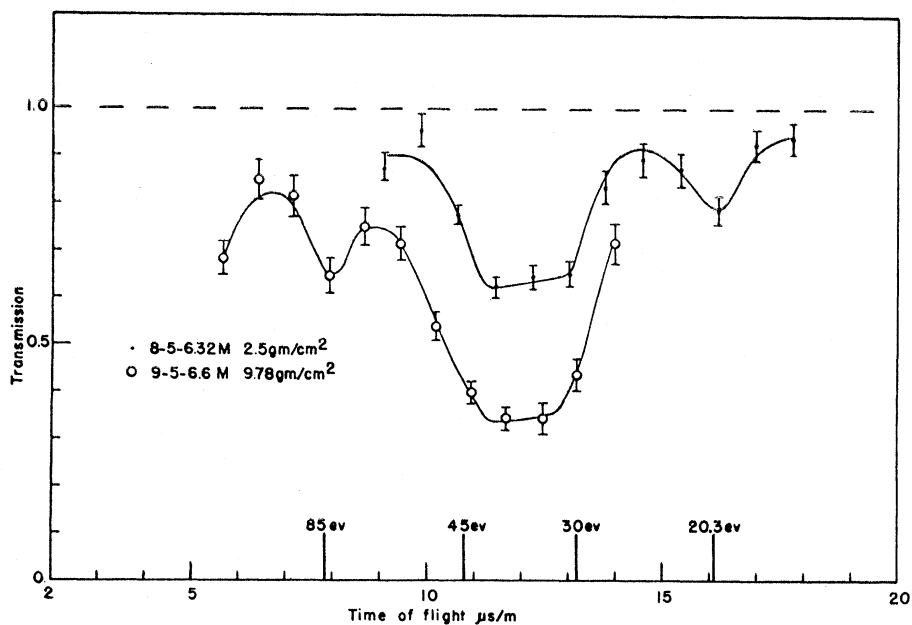
FIG. 8. Observed transmission of I absorbers at high energy.
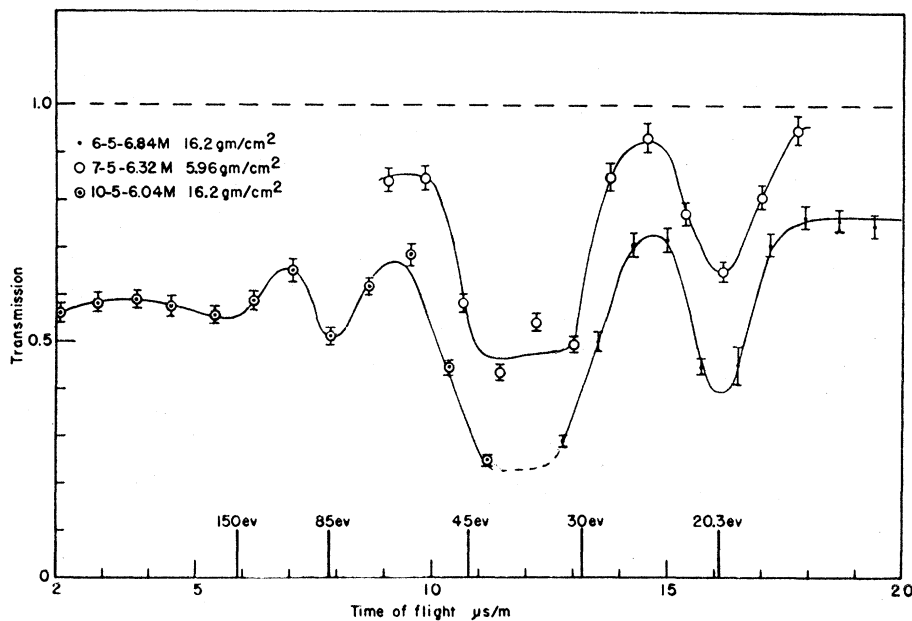
FIG. 9. Observed transmission of I absorbers at high energy.

tion is necessary, at least for the most interesting part of the curve, because the transmission varies nearly linearly with time of flight within a resolution width, and if the transmission is linear with time of flight, the measured transmission is equal to the actual transmission.

Breaks in the curve are noted at times of flight of 970 μs/m and 1200 μs/m, corresponding to neutron wave-lengths of 3.9 and 4.8A, respectively, which were interpreted as the effect of the crystalline structure of iodine on the scattering cross section. Except for the crystalline

effects, the points lie very nearly on a straight line, thus verifying the 1/v absorption law. The equation for the best straight line through the points, excluding the crystalline effects, is given by $\sigma = (3.6+0.0146t) \times 10^{-24}$ cm^2/atom, where t is the time of flight in μs/m and σ is the cross section. This is the same as $\sigma = (3.6+1.06E^{-\frac{1}{2}}) \times 10^{-24}$ cm^2/atom, where E is the energy in ev. The error in the slope of this curve is believed to be no more than 4 percent. The intercept of this curve is taken as the scattering cross section at the energies above 0.5 ev. At energy kT (0.025 ev), $\sigma = 10.3 \times 10^{-24}$ cm^2/atom.

Figure 7 shows the time-of-flight region between the low energy resonance and 100 μs/m. Again, no correction has been made for the effect of the resolution function on the cross section. The statistical errors are shown in the usual manner. The dotted straight line has the same slope and intercept as the straight line which best fits the data shown in Fig. 6.

Figures 8 and 9 show the measured transmission as a function of time of flight for the data taken above 14 ev. Data were taken with several thicknesses of absorber in order to determine the character of the resonances indicated in these figures. The curves through the points

serve to indicate the probable shape of the transmission curve as seen by the spectrometer. The curves indicate that there is a single absorption resonance near 16 μs/m. The flat region of low transmission of the curves between 11 and 12 μs/m contains a number of unresolved resonances. At 8 μs/m there is an indication of another resonance or group of resonances. At higher energies, there are indications of other resonances.

In a region where the transmission varies non-linearly by a large amount within a resolution width of the apparatus, it is expected that large corrections have to be made in the data to obtain the true transmission of the absorber. With the best resolution used with the present apparatus there are large variations in the cross section of iodine within a resolution width, in the region of the resonances. The variation in the transmission can be reduced by making the absorber thin, but it is very difficult to obtain a good indication of the cross section from the measured transmission of a very thin absorber. One can obtain some information on the character of the cross section by measuring the transmission for several thicknesses of the absorber as was done in the region of the resonances.
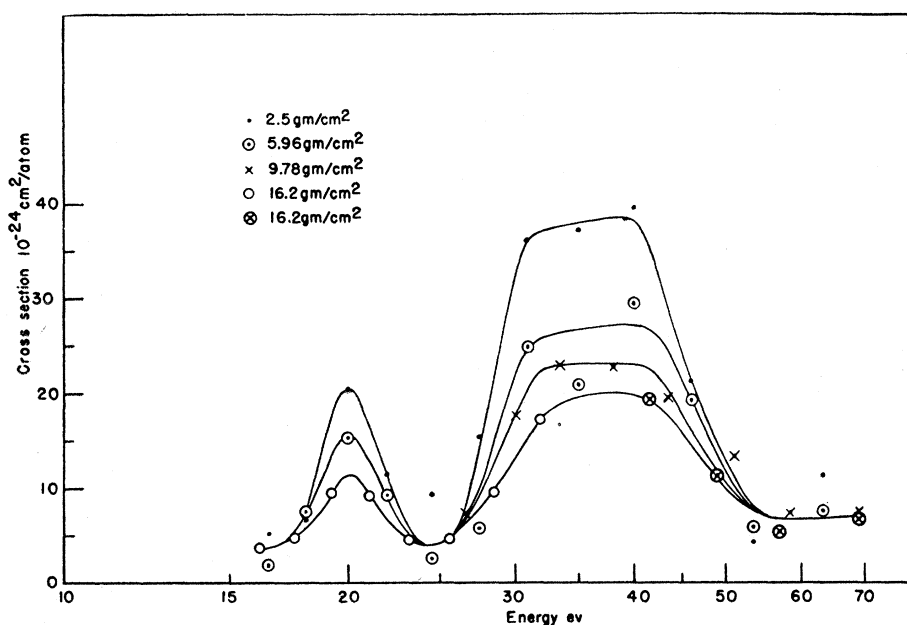
FIG. 10. Cross section of I in the region of the main resonances calculated from the formula $T = \exp(-\sigma n)$, with no correction for apparatus resolution.
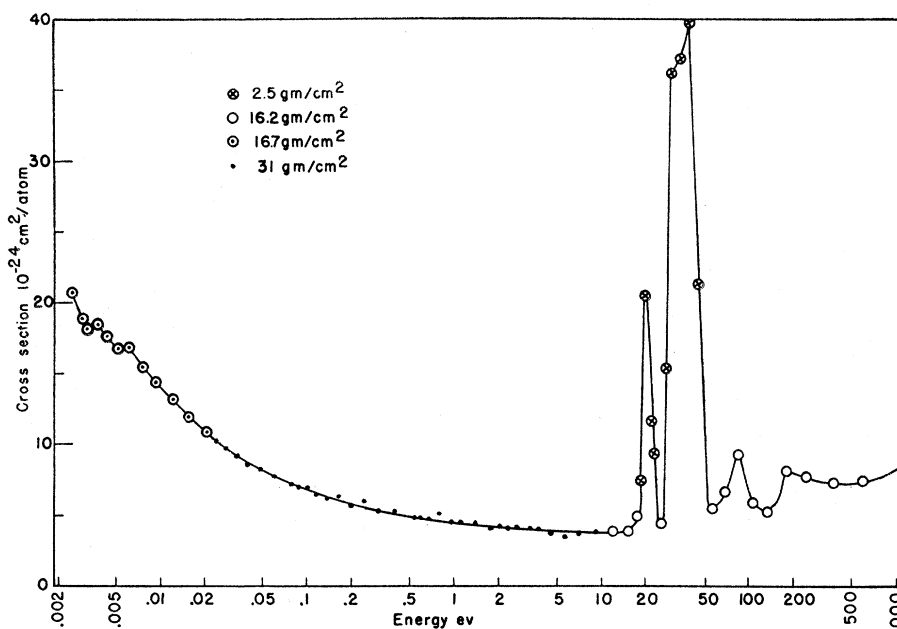
FIG. 11. Cross section of I as a function of neutron energy for the energy region studied. No correction has been made for apparatus resolution.

Figure 10 demonstrates the effect of changing the absorber thickness in transmission measurements. The cross section was obtained from the observed transmission in the formula $T = \exp(-\sigma n)$, where T is the transmission and n is the absorber thickness in atoms/cm². The cross section thus obtained is plotted as a function of the logarithm of the energy. It is noted that the apparent cross section increases with decreasing absorber thickness in the region of the resonances, as is expected. Thus the best indication of the cross section in the region of the resonances is given by the thinnest absorber. One fact demonstrated by this graph is that there are large variations in the cross section within a resolution width in the energy region between 30 and 45 ev, where the spectrometer indicates little variation. Of course, in regions where there are no large variations of cross section within a resolution width, the cross section is given best by the thick absorber data.

Figure 11 shows a plot of the cross section as a function of energy for the whole energy range investigated, the abscissa having a logarithmic scale. Only those data are plotted which give the best representation of the cross section in the regions where data were taken for several thick-

nesses of absorber. However, it must be remembered that in the region of the resonances the best measured values of the cross section are subject to large corrections because of the finite resolution width. Using a logarithmic energy scale shows the data in such a way that the resolution width is the same order of magnitude over the whole energy range.

5. DISCUSSION

For the most part, this discussion is concerned with the treatment of the data in the region of the resonances. In the region below 15-ev neutron energy the variations in the cross section are sufficiently slow (except for the crystalline effects) so there is no significant difference between the actual transmission and the observed transmission of an absorber. In the region of the resonances the corrections required in the observed transmission to obtain the actual transmission are very large.

Baker and Bacher[3] have given a treatment of the problem of obtaining the transmission curve for an absorber from the transmission observed with a slow neutron velocity spectrometer. They demonstrate that it is rather difficult to proceed directly from the observed transmission to the

actual transmission of an absorber. A much simpler procedure is to assume a certain transmission, find the effect of the resolution of the apparatus on the assumed transmission, and compare this result with the observed transmission. This process is repeated until a good comparison with the experimentally determined transmission is found. In the region of a resonance, the transmission assumed is that obtained from the Breit-Wigner single-level formula[6] with a correction for the Doppler effect, and the parameters in the formula are adjusted for the best correspondence to the observed data.

The resolution function is the sensitivity of the apparatus, for any one channel, as a function of the neutron time of flight. If the resolution function were determined solely by the on-times, its shape would be that of an isosceles triangle with the base of the triangle twice the on-time. However, several other factors influence the shape of the resolution function. The combined effect of the on-time of the arc and detector channels, the straggling in the arrival of deuterons at the Be target, and the uncertainty in the time of detection caused by the finite rise time of the linear amplifier is shown by the FN-function. A typical FN-function is shown in Fig. 5 for an on-time of 5 μs. It is seen that by far the largest contribution to the spread of the FN-function is the on-time.

Contributions to the spreading of the resolution not measured by the FN-function are the uncertainty of the time spent by the neutrons in the moderator, the uncertainty in the source position, and the uncertainty in the position of the detection of the neutrons in the BF_3 chamber. Under the conditions of interest here, i.e., for neutron energies greater than 15 ev and distances of flight greater than six meters, only the last of these three contributions is of significance. The neutrons are almost equally likely to be captured at any point along the 15-cm length of the BF_3 chamber. The time required for a 20-ev neutron to traverse 15 cm is 2.4 μs. The uncertainty in the source position is less than one centimeter, and this is small compared with 15 cm. The uncertainty in the time of the neutrons in the moderator is a few tenths of a microsecond, and this is small com-

pared with the time for a neutron to traverse the chamber length. Therefore, the resolution function is determined essentially by the FN-function and the simple step-function representing the sensitivity of the apparatus as a function of distance.

Figure 12a shows the apparatus resolution function for an on-time of 5 μs, a source-detector distance of 6.5 meters, and for 20-ev neutrons. In making comparisons between the Breit-Wigner formula and the data, it is convenient to use a step-function approximation for the resolution function. Figure 12b shows the step-function approximation used for the resolution function shown in Fig. 12a. The step-function is made symmetrical with respect to the line corresponding to zero time. Also, the second moment of the step-function taken at zero time is made equal to the second moment of the resolution function taken with respect to the vertical line through its centroid.

A symmetrical form of the Breit-Wigner single-
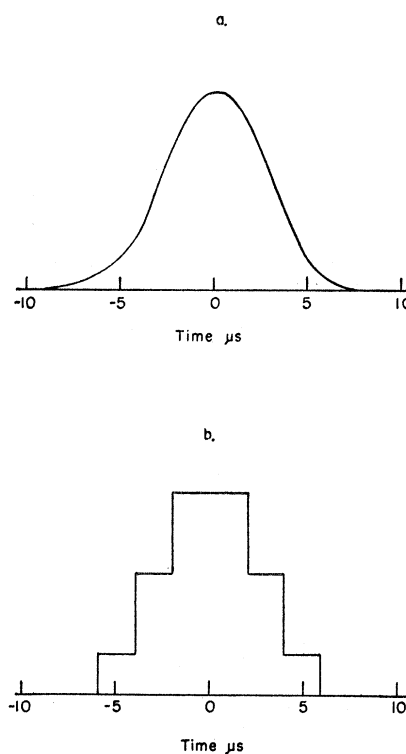
FIG. 12(a). Apparatus resolution function for 5 μs on-time, 20-ev neutrons, and 6.5-m distance of flight. (b). Step-function approximation for resolution function above.

[6] H. Feshbach, D. C. Peaslee, and V. F. Weisskopf, Phys. Rev. **71**, 145 (1947).
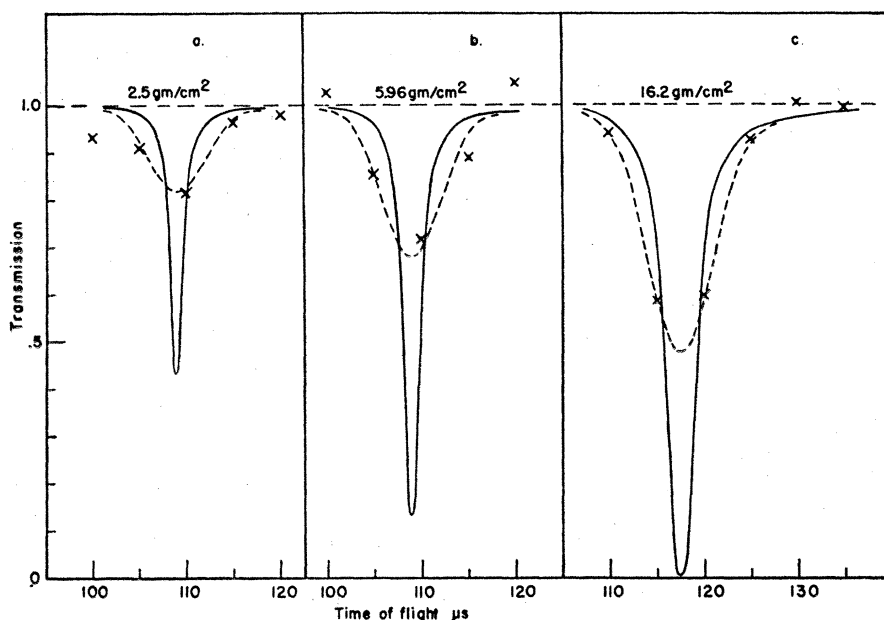
Fig. 13. Comparison of the Breit-Wigner formula with experimental points for three
thicknesses of absorber used for the 20.3-ev resonance.

level formula was used of the following form:

$$\sigma_a(E) = \frac{\sigma_0 \Gamma^2}{\Gamma^2 + 4(E - E_r)^2},$$

where σ_a = neutron cross section, E = neutron
energy, E_r = resonance energy, σ_0 = cross section
at resonance, and Γ = level width. The cross section
given by this formula is modified by the Doppler
effect resulting from the thermal motion of the
absorber atoms. Thus the effective cross section
is given by

$$\sigma(E) = (1/\pi^{\frac{1}{2}}\Delta) \int_{-\infty}^{\infty} \sigma_a(E')$$

$$\times \exp[-(E-E')^2/\Delta^2] dE',$$

where $\Delta = 2(E_r E_{th} m/M)^{\frac{1}{2}}$ = Doppler width,
m = neutron mass, E_{th} = thermal energy, M = mass
of target nucleus. Since the Debye temperature
for iodine is 106°K, the thermal energy is taken
as kT, in accordance with the calculation by
Lamb,[7] to take into account the lattice binding.
The value of Δ is then 0.13 ev for $E_r = 20$ ev.

The low energy resonance is now considered. In

[7] W. E. Lamb, Phys. Rev. 55, 190 (1939).

order to make a comparison between a theoretical
curve and an observed transmission, the ob-
served transmission curve must be corrected for
the scattering cross section. The value of the
cross section obtained by extrapolating the curve
which gives the best fit in the 1/v region, to zero
time of flight, is used as the scattering cross
section. Thus the observed transmission in the
region of the resonance was divided by the trans-
mission corresponding to a scattering cross sec-
tion of 3.6×10^{-24} cm^2/atom. Values are chosen
for the parameters of the Breit-Wigner formula
to give σ_a. From σ_a, σ is then determined. For
each absorber thickness, σ was used to determine
the transmission as a function of time of flight for
the source-detector distance used in taking the
data under consideration. The step-function ap-
proximation to the resolution function is then
used to obtain the transmission curve due to
absorption that would be observed for a cross
section given by the Breit-Wigner formula with
the chosen parameters. Such transmission curves
were compared with the observed curves and
parameters adjusted until the best correspond-
ence was obtained.

Figure 13a, b, and c shows the transmission
curves obtained from the theory with a particular

set of parameters which gives the best correspondence to the observed data for the three absorber thicknesses used on the low energy resonance. The solid curves are the transmissions given by the theory, the dotted curves are these transmissions after being put through the resolution function, and the crosses show the experimental data corrected for the scattering cross section. The values of the parameters giving this correspondence are $E_r = 20.3$ ev, $\sigma_0 = 80 \times 10^{-24}$ cm^2/atom, $\Gamma = 0.45$ ev. The error in E_r is about 0.5 ev. Because of the magnitude of the experimental errors, the values of σ_0 and Γ may be varied over quite a wide range, with correspondence between the theory and experiment within the experimental error. Also, because of the Doppler effect, no minimum value of Γ or maximum value of σ_0 can be given. The maximum value of Γ and minimum value of σ_0, which give a theoretical curve which could be said to correspond to the experimental points, are 0.8 ev and 40×10^{-24} cm^2/atom, respectively.

Another method of analysis which is useful yields information on the values of the parameters in the Breit-Wigner formula, and is largely independent of the resolution of the apparatus. The method has to do with the behavior of the activity integral for a resonance as a function of absorber thickness. The activity, I, for a resonance and a particular absorber thickness is given by

$$I = \int (1 - T)dy,$$

where T is the transmission of the absorber as a function of time of flight t, and $dy = dt/t_r$, where t_r is the time of flight corresponding to the E_r for the resonance. The limits of the integral are taken as values of t on either side of the resonance where $T \approx 1$. For a given absorber thickness the value of I is the same for any resolution that is used to measure T if the resolution is sufficiently good to separate the resonance in question from other resonances.

If the symmetrical form of the Breit-Wigner formula is used, then

$$I = \int_{-\infty}^{\infty} \left[1 - \exp\left(-\frac{n\sigma_0\Gamma^2}{\Gamma^2 + 4(E - E_r)^2} \right) \right] dy.$$

If $n\sigma_0$ is sufficiently small so that the exponential term in the integrand may be approximated by the first two terms of a power series, then

$$I = \pi n \Gamma \sigma_0 / 4E_r.$$

No error is made in this equation by neglecting the Doppler effect. Thus the activity is proportional to the absorber thickness for thin absorbers.

If $n\sigma_0 \gg 1$, little error is made by assuming $\Gamma^2 \ll (E - E_r)^2$ in computing the activity using the Breit-Wigner formula. Making this approximation, one obtains

$$I = (\pi n \Gamma^2 \sigma_0)^{\frac{1}{2}} / 2E_r.$$

Thus for thick absorbers, the activity is proportional to the square root of the absorber thickness.

If the apparatus resolution is so wide that levels cannot be resolved, if $n\sigma_0 \gg 1$ for each level, and if the separation of the levels is large compared with the level widths (as must be the case for the Breit-Wigner formula to hold).

$$I = (n\pi)^{\frac{1}{2}} \sum_r (\sigma_{0r}\Gamma_r{}^2/4E_r{}^2)^{\frac{1}{2}},$$

where r denotes parameters characterizing the rth level, and the sum is taken over the unresolved group. Again, for thick absorbers, the activity is proportional to the square root of the absorber thickness. The Doppler effect introduces an error in all these formulas for I for thick absorbers. However, if $\Delta \ll \Gamma_r$ for the resonances or if the absorber is sufficiently thick, the error is negligible.

In Fig. 14a is shown a plot of activity calculated from the experimental curves (corrected for scattering cross section) as a function of the square root of the absorber thickness for the low energy resonance. With the possible exception of the point for the thinnest absorber, these points fall very nearly on a straight line. From the slope of this curve, one finds that $\sigma_0\Gamma^2 = 15 \times 10^{-24}$ ev^2 cm^2/atom, assuming no error to be introduced by the Doppler effect. This is in agreement with the value of 17×10^{-24} ev^2 cm^2/atom, by use of the values of σ_0 and Γ obtained from the curve-fitting method described above. The Doppler effect is neglected because an analysis taking into account this effect is difficult, and the data are
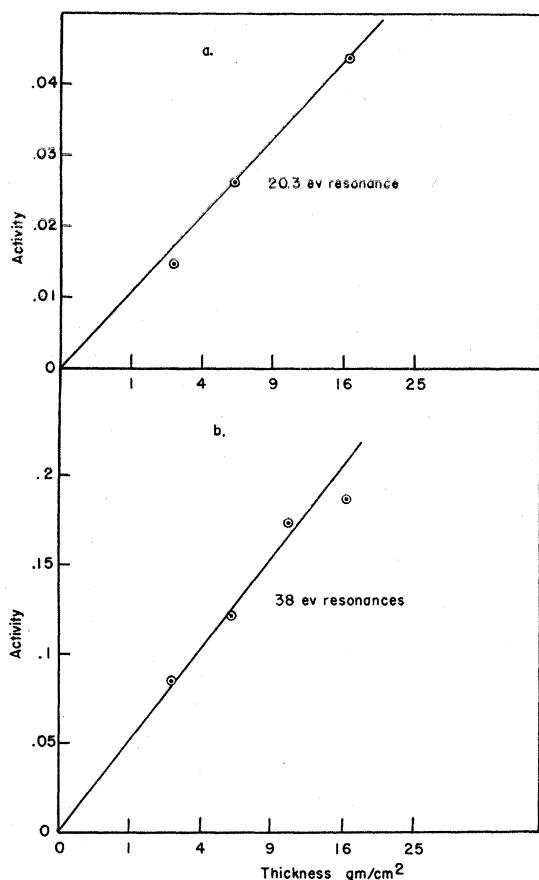
FIG. 14. Activity vs. square root of absorber thickness.

not sufficiently accurate to warrant this refinement of the analysis.

The energy region 25 to 50 ev is now considered. If the cross section were constant between 30 and 40 ev, the apparatus resolution is sufficiently good so that the measured transmission would be an exponential function of the thickness. That this is not the case is demonstrated in Fig. 10. Therefore, it may be concluded that the 25- to 50-ev region must contain at least two resonances. By making use of the curve-matching method it was not found possible to fit two resonance curves of about equal $\sigma_0\Gamma^2$ to the data for all thicknesses of absorber used. One sees that this is evidently the case from two considerations. The width of the dips in the transmission curves are about the same for all thicknesses of absorber. This indicates that there must be narrow resonances near the edges of the dip in transmission. However, two narrow resonances

near the edges of the dip would not give a flat bottom to the dip for the thick as well as the thin absorbers. Therefore it is concluded that in this energy region there are at least 3 resonances. No attempt was made at curve matching to determine the characteristics of 3 resonances that might fit the data, because there are insufficient data to justify such an attempt. There is no method of deducing from the data the maximum number of resonance levels in this energy region.

Shown in Fig. 14b is a plot of activity for the 25- to 50-ev region as a function of the square root of the absorber thickness. The points fall very nearly on a straight line, indicating that the absorbers are thick for all or most of the resonances in this region. One finds from this curve that $\sum_r (\sigma_{0r}\Gamma_r^2)^{\frac{1}{2}}$ for the resonances is 32.5×10^{-12} ev-cm/atom$^{\frac{1}{2}}$. This value is given under the assumption that 38 ev is near the resonance energy for each resonance and that no error is introduced by the Doppler effect.

The data on the 25- to 50-ev region are now reviewed to determine what evidence exists for believing that the resonances in this region have widths of the order expected from the theory. It is assumed that the Breit-Wigner formula holds for these resonances. This means that the widths of the resonances must be small compared with the spacing. If, for example, it is supposed that there are 3 levels with about 10-ev spacing of about equal strengths, $\sigma_0\Gamma^2=120\times10^{-24}$ ev^2 cm^2/atom for each level. The data indicate that σ_0 for such resonances is large compared with 40×10^{-24} cm^2/atom. Thus, for this possible distribution of levels, the widths are no greater than 1 ev. If it is supposed that there are 3 levels unequally spaced, then the levels nearest each other must be weak and narrow because of their small spacing, and the third level could have $\sigma_0\Gamma^2$ as large as 200×10^{-24} ev^2 cm^2/atom corresponding to a width perhaps as great as 2 ev. Thus, to correspond to the data, no one of the three supposed levels could have a width of more than 1 or 2 ev. If it is supposed that there are four or more resonances within this region, it is evident that the level widths can be no more than 1 or 2 ev. The conclusions drawn above are based on the assumption that $\Gamma\gg\Delta$. On the other hand, the level widths may be about the same as, or smaller than, the Doppler width, $\Delta=0.19$ ev, at

this energy. However, if this is so, then one is led to the same conclusion, namely, that abnormally wide levels are not indicated by the data.

With regard to the energy region above 60 ev, little can be said about the constants of the resonances. It seems evident that there is at least one resonance in the neighborhood of 85 ev. However, the resolution of the apparatus is not sufficiently good at this and higher energies to make it possible to obtain more information than this from the data.

Because of the fact that the iodine resonances occur at rather high energies, it is not expected that the data obtained by indirect methods should compare well with the present data. The recently reported results of Wu, Rainwater, and Havens,[2] using the Columbia neutron spectrometer on iodine, agree with the results obtained here with regard to the energies for the resonance absorption and with regard to the slope and intercept for the best straight-line fit for the data in the low energy region. However, their result for the value for $\sigma_0\Gamma^2$ of about 4×10^{-24} ev^2 cm^2/atom for the 20.3-ev resonance is only $\frac{1}{4}$ the value ob-

tained here. They assume that the 38-ev group of resonances is composed of two levels of equal strengths with $\sigma_0\Gamma^2 = 135\times10^{-24}$ ev^2 cm^2/atom. In the present experiment it is found that there must be at least three resonances in the 38-ev region. If it is assumed that there are only three resonances of equal strength, the data presented here indicate that $\sigma_0\Gamma^2 = 115\times10^{-24}$ ev^2 cm^2/atom for each resonance level. Using their data and postulating three levels of equal strength, one obtains $\sigma_0\Gamma^2 = 60\times10^{-24}$ ev^2 cm^2/atom. There is no apparent reason for these discrepancies unless an error has been made or unless the resolution of their apparatus is not sufficiently good to separate the resonance groups in the particular way they are separated in the present experiment.